

EFFECTS OF MAGNETOMETER CALIBRATION AND MANEUVERS ON ACCURACIES OF MAGNETOMETER-ONLY ATTITUDE-AND-RATE DETERMINATION*

M. Challa[†] and G. Natanson[†]

ABSTRACT

Two different algorithms—a deterministic magnetic-field-only algorithm and a Kalman filter for gyroless spacecraft—are used to estimate the attitude and rates of the Rossi X-Ray Timing Explorer (RXTE) using only measurements from a three-axis magnetometer. The performance of these algorithms is examined using in-flight data from various scenarios. In particular, significant enhancements in accuracies are observed when the telemetered magnetometer data are accurately calibrated using a recently developed calibration algorithm. Interesting features observed in these studies of the inertial-pointing RXTE include a remarkable sensitivity of the filter to the numerical values of the noise parameters and relatively long convergence time spans. By analogy, the accuracy of the deterministic scheme is noticeably lower as a result of reduced rates of change of the body-fixed geomagnetic field. Preliminary results show the filter-per-axis attitude accuracies ranging between 0.1 and 0.5 deg and rate accuracies between 0.001 deg/sec and 0.005 deg./sec, whereas the deterministic method needs a more sophisticated techniques for smoothing time derivatives of the measured geomagnetic field to clearly distinguish both attitude and rate solutions from the numerical noise. Also included is a new theoretical development in the deterministic algorithm: the transformation of a transcendental equation in the original theory into an 8th-order polynomial equation. It is shown that this 8th-order polynomial reduces to quadratic equations in the two limiting cases—infinately high wheel momentum, and constant rates—discussed in previous publications.

INTRODUCTION

It has been demonstrated¹⁻¹⁰ that the attitude and rates of low-Earth orbiting spacecraft can be simultaneously estimated using measurements of the Earth's magnetic field, \vec{B} , using only a three-axis magnetometer (TAM) and *no a priori* information. The feasibility of this "TAM-Only" scheme essentially

* This work was supported by the National Aeronautics and Space Administration (NASA) / Goddard Space Flight Center (GSFC), Greenbelt, Maryland, Contract GS -35F-4381G, Task Order No. S-03365-Y.

[†] Computer Sciences Corporation, 10110 Aerospace Road, Lanham-Seabrook, MD 20706

relies upon \bar{B} changing direction rapidly enough in the spacecraft body frame to make computation of its time derivative possible, and these changes during the course of an orbit are sufficiently large to enable determination of all three Euler angles using only TAM data.

Our approach consists of using two independent algorithms—deterministic attitude determination from magnetometer-only data (DADMOD) and the Real Time Sequential Filter (RTSF). The DADMOD¹⁻³ is a TAM-only algorithm that relates the time derivatives of \bar{B} in inertial and spacecraft body coordinates to determine the attitude and the body rates. The RTSF⁴⁻⁵ is a robust Kalman filter that estimates, in addition to the attitude, errors in rates propagated via Euler's equation. Note that the RTSF is a general algorithm for gyroless spacecraft; however, its sensitivity to rate errors as small as 0.0003 deg/sec makes it a robust and accurate real-time algorithm even in TAM-only situations with no *a priori* spacecraft information.

The highlights of our past applications to in-flight data from the Solar, Anomalous, and Magnetospheric Explorer (SAMPEX) and the Earth Radiation Budget Satellite (ERBS) have shown that with a TAM-Only approach: (1) SAMPEX attitude and rate requirements can be met even when the on-board Sun sensor fails⁴⁻⁶, (2) using partially calibrated magnetometer data from ERBS nominal mission mode the RTSF yields⁸ accuracies within 0.4 deg and rate accuracies within 0.005 deg/sec, and (3) ERBS attitude and rates could be reliably determined¹⁰ during its 1987 control anomaly¹¹ when the spacecraft tumbled at approximately 2 deg/sec. Another useful aspect of the past work is the combination of the strengths of these algorithms in an automated scheme wherein the deterministic algorithm is used to initialize the more accurate Kalman filter to within a few degrees of the correct spacecraft attitude.

In the present work, we examine the performances of these algorithms during some important scenarios of the RXTE: (1) calibrated and uncalibrated TAMs and (2) during maneuvers. While the first scenario does not require further explanation, the motivation for the second is the possible application of the RTSF to extend aging missions. For example, ERBS (launch: 1984) needs monthly thruster-based maneuvers for solar-power purposes, and these are currently conducted using rate information from the one remaining gyro channel. This paper demonstrates that, by providing magnetometer-only rate solutions, the filter can be a useful tool during such maneuvers, especially when the last gyro channel also fails.

The present work concentrates on results for RXTE that are interesting in their own right, because, in contrast to SAMPEX and ERBS:

- RXTE is inertial pointing so that \bar{B} changes very slowly in the body frame, and this leads to observability and convergence issues when only short data spans are used (as is the case here).
- RXTE is a zero-momentum spacecraft, whereas SAMPEX and ERBS are momentum-biased about the pitch axis. We believe this leads to the RTSF results being very sensitive to the numerical values of its propagation noise parameters and their relationship to the weightage of the TAM data. For a similar reason, the accuracy of the deterministic scheme becomes noticeably lower.

The rest of the paper is organized as follows. Section 2 briefly describes the algorithms; included here are recent developments in DADMOD and a novel TAM calibration algorithm¹² that is used to calibrate the RXTE TAM data. Sections 3 and 4 analyze the performances for RXTE and ERBS respectively, and Section 5 summarizes the conclusions.

ALGORITHMS

Deterministic Attitude and Rate Determination Using Magnetometer-Only Data (DADMOD)

As discussed in detail in previous publications, determination of the spacecraft attitude and rates based on magnetometer measurements and their first and second time derivatives can be cast in the form of the following vector equation:

$$\bar{\Lambda}_0(\Phi) + \bar{\Lambda}_1(\Phi) \omega_1 + \bar{\Lambda}_2 \omega_1^2 = \bar{\theta} \quad (1)$$

where the angle Φ and the body rate ω_1 around the body-fixed geomagnetic field vector $\bar{\mathbf{B}}^A$ are two unknown variables. It is essential that

$$\bar{\Lambda}_1(\Phi) \equiv \hat{\mathbf{B}}^A \times \bar{\mathbf{H}}_1(\Phi), \quad \bar{\Lambda}_2 \equiv \bar{\Omega}_2 \times \bar{\mathbf{B}}^A, \quad (2)$$

where the vectors $\bar{\mathbf{H}}_1(\Phi)$ and $\bar{\Omega}_2$ are given by Eqs. (5) and (6) in Ref. 10, and $\hat{\mathbf{B}}^A \equiv \bar{\mathbf{B}}^A / |\bar{\mathbf{B}}^A|$. The third vector $\bar{\Lambda}_0(\Phi)$ is also perpendicular to $\bar{\mathbf{B}}^A$ at any value of the angle Φ so that two nontrivial equations to determine both Φ and ω_1 are obtained by projecting vector equation (1) on two directions perpendicular to the geomagnetic field. As a new development, we show that these two directions can be chosen in such a way that $\zeta(\Phi) = \tan(\Phi/2)$ becomes one of roots of an 8th-order polynomial $P_8[\zeta]$.

In fact, by projecting Eq. (1) onto the vector $\bar{\mathbf{B}}^A \times \bar{\Lambda}_2$ one finds

$$\omega_1(\Phi) = - |\bar{\mathbf{B}}^A| (\bar{\Lambda}_0(\Phi) \cdot \bar{\Omega}_2) / (\bar{\mathbf{H}}_1(\Phi) \cdot \bar{\Lambda}_2) \quad (3)$$

Substituting the latter expression into the projection of Eq. (1) onto the vector $\bar{\mathbf{H}}_1(\Phi)$ then gives

$$(\bar{\mathbf{H}}_1(\Phi) \cdot \bar{\Lambda}_2) (\bar{\Lambda}_0(\Phi) \cdot \bar{\mathbf{H}}_1(\Phi)) + |\bar{\mathbf{B}}^A|^2 (\bar{\Lambda}_0(\Phi) \cdot \bar{\Omega}_2)^2 = 0 \quad (4)$$

It can be shown that the vectors $\bar{\Lambda}_0(\Phi)$ and $\bar{\mathbf{H}}_1(\Phi)$ have the form:

$$\bar{\Lambda}_0(\Phi) = c^4(\Phi) \bar{\mathcal{Q}}_4[\zeta(\Phi)], \quad \bar{\mathbf{H}}_1(\Phi) = c^2(\Phi) \bar{\mathcal{Q}}_2[\zeta(\Phi)] \quad (5)$$

where the vectors $\bar{\mathcal{Q}}_n[\zeta]$ are formed by polynomials of the n^{th} order in ζ and $c(\Phi) \equiv \cos(\Phi/2)$, and therefore the solution sought for is given by one of roots of the 8th-order polynomial:

$$P_8[\zeta] \equiv P_2[\zeta] P_6[\zeta] + (P_4[\zeta])^2 \quad (6)$$

where

$$P_2[\zeta] \equiv (\bar{\mathcal{Q}}_2[\zeta] \cdot \bar{\Lambda}_2), \quad P_4[\zeta] \equiv |\bar{\mathbf{B}}^A| (\bar{\mathcal{Q}}_4[\zeta] \cdot \bar{\Omega}_2), \quad P_6[\zeta] \equiv (\bar{\mathcal{Q}}_2[\zeta] \cdot \bar{\mathcal{Q}}_4[\zeta])$$

Note that all coefficients of polynomial (6) are equal to zero when the geomagnetic field is directed along one of the spacecraft principal axes of inertia since both vectors $\bar{\Omega}_2$ and $\bar{\Lambda}_2$ vanish. By analogy these coefficients are nullified if the vector $\bar{\Lambda}_2$ becomes perpendicular to the vector $\bar{\mathbf{H}}_1(\Phi_1)$ for the sought-for root $\zeta(\Phi_1)$. However, it can be shown that the ratio $(P_4[\zeta])^2 / P_2[\zeta]$ tends to zero in both cases so that the solution sought for can be found among real roots of the polynomial $P_6[\zeta]$. Because Eq. (3) is no longer applicable, one has to solve a quadratic equation to find ω_1 . To avoid instabilities, a special algorithm was developed to select the direction associated with the maximum of the discriminant. As a result, the resultant solution remains stable as the coefficient of the quadratic term tends to zero.

The ratio $(P_4[\zeta])^2 / P_2[\zeta]$ also vanishes as the wheel momentum \vec{h} tends to ∞ , while the polynomial $P_6[\zeta]$ takes the form:

$$P_6[\zeta] \approx (1 + \zeta^2)^2 \Pi_2[\zeta] \quad (7)$$

As a result, we come to the quadratic equation $\Pi_2[\zeta] = 0$ discussed in Ref. 6. A similar decomposition of the polynomial $P_6[\zeta]$ takes place in case of constant body rates after one drops all terms associated with the time derivative of the angular velocity vector $\vec{\omega}$. The solution solved for can be found from the requirement for the vectors $\vec{H}_1(\Phi)$ and $\vec{A}_0(\Phi)$ to be perpendicular to each other, which is equivalent to the condition $P_6[\zeta(\Phi)] = 0$. The resultant quadratic equation $\Pi_2^0[\zeta] = 0$ has been studied in detail in Refs. 1 and 2.

Real Time Sequential Filter (RTSF)

In view of space considerations, only details relevant to the tuning of the RTSF are presented here. A full mathematical description of the RTSF has been provided elsewhere (References 4 and 5). The RTSF's state vector \vec{X} is comprised of the four components of the attitude quaternion, \vec{q} , and the corrections, \vec{b} , to the spacecraft's rates, $\vec{\omega}$:

$$\vec{X} = [\vec{q}^T \vec{b}^T]^T \quad (8)$$

(Note that the components of \vec{b} and $\vec{\omega}$ are resolved along the spacecraft's x, y, z axes.)

The RTSF uses sensor data to estimate \vec{q} as well as \vec{b} , with \vec{b} being estimated kinematically in the same manner as gyro biases for a gyro-based spacecraft; i.e., by attributing differences between the measured and propagated attitudes to errors in $\vec{\omega}$. The \vec{b} estimates are then used to correct $\vec{\omega}$, and these corrected rates are used as initial conditions to propagate Euler's equation to the next measurement time. The propagation of \vec{b} is modeled via a first-order Markov model:

$$\frac{d\vec{b}}{dt} = -\frac{\vec{b}}{\tau} + \vec{\eta}_b \quad (9)$$

where $\vec{\eta}_b$ is a white noise term, and τ is a finite time constant. A suitable value for τ is the time between measurements.

The rates are assumed to contain a white noise component, $\vec{\eta}_a$ and are propagated using Euler's equation after accounting for the angular momentum contributed by the wheels, and for the total external torques acting on the spacecraft. TAMONLY currently models the gravity-gradient torque and the magnetic control torque acting on the spacecraft. (The aerodynamic drag torque and the radiation pressure torque have been intentionally omitted to reduce the amount of spacecraft modeling required. The RTSF relies on the rate-corrections, \vec{b} , to compensate for the small effects of these torques.)

The covariance matrix, P , is propagated by numerically integrating the following equation:

$$\frac{dP}{dt} = F(\vec{\omega})P + P F^T(\vec{\omega}) + Q \quad (10)$$

Here $F(\bar{\omega})$ is described in Reference 5; the quantity of interest is the 6×6 matrix Q that quantifies the propagation noise and is of the following diagonal form:

$$Q = \text{diag} [Q_a, Q_a, Q_a, Q_b, Q_b, Q_b] \quad (11)$$

Here Q_a is related to the noise term $\bar{\eta}_a$ and contributes to the growth of the attitude error covariances about the body X-, Y-, and Z-axes during propagation. Similarly, Q_b is related to noise term $\bar{\eta}_b$, and contributes to the growth of the error covariances of \bar{b} during propagation. Another quantity that we must consider during tuning is σ , the strength of the white noise in the TAM measurements.

The filter can be initialized in one of the following two ways before processing a span of telemetry data.

- Inertial initial conditions (IIC), where the spacecraft is assumed at rest in the Geocentric Inertial Coordinates (GCI) with its axes coinciding with the GCI axes; this results in large initial errors.
- Deterministic initial conditions (DIC) where the filter makes short (2 to 5 min) runs and determines which of the DADMOD solutions is a good *a priori* solution. This results in small initial errors.

The TAM Calibration Algorithm

The effects of TAM calibration were determined using a recently-developed algorithm¹² where the following set of 21 time-independent parameters are used to "adjust" the magnetic field vector measured by the TAM whose axes nominally coincide with the spacecraft body axes.

- E 3x3 scale factor/misalignment matrix nominally equal to the identity matrix, $I_{3 \times 3}$
- G 3x3 TAM-torquer coupling matrix nominally equal to the null matrix, $O_{3 \times 3}$
- \bar{f} 3x1 bias vector nominally equal to the null vector, $O_{3 \times 1}$

If at any instant \bar{B} is the magnetic field vector measured by the TAM, \bar{D} is the 3x1 dipole moment vector of the magnetic torquer bars, A is the *known* GCI -to-spacecraft body frame attitude matrix, and \bar{B}_i^R is the corresponding International Geomagnetic Reference Field (IGRF)¹³ vector in the inertial frame, the calibration model assumes

$$B_i = \sum_{j=1}^3 (E_{ij} B_j^R - G_{ij} D_j) - f_i + v_i, \quad i = 1, 2, 3 \quad (12)$$

where $\bar{B}^R = A\bar{B}_i^R$ is the predicted field in the spacecraft body frame, and \bar{v} is a white-noise term of root-mean-square (r-m-s) value σ . The goal of the calibration then is to estimate E , G , and \bar{f} , by applying statistical methods to a span of TAM measurements, $\{\bar{B}_1, \dots, \bar{B}_N\}$ and the corresponding predictions $\{\bar{B}_1^R, \dots, \bar{B}_N^R\}$.

Resolving E and G into the vectors $\bar{E}_1, \bar{E}_2, \bar{E}_3, \bar{G}_1, \bar{G}_2,$ and \bar{G}_3 as follows,

$$E = \begin{bmatrix} \bar{E}_1^T \\ \bar{E}_2^T \\ \bar{E}_3^T \end{bmatrix}, \quad G = \begin{bmatrix} \bar{G}_1^T \\ \bar{G}_2^T \\ \bar{G}_3^T \end{bmatrix}, \quad (13)$$

three independent loss functions are now formulated as:

$$L_i = \frac{1}{\sigma_{T,i}^2} \sum_{n=1}^N a_{n,i} \left[\bar{E}_i^T \bar{B}_n^R - \bar{G}_i^T \bar{D}_n - f_i - B_{n,i} \right]^2, \quad i = 1, 2, 3 \quad (14)$$

where the subscript n denotes the measurement time,

$$\frac{1}{\sigma_{T,i}^2} = \sum_{n=1}^N \frac{1}{\sigma_{n,i}^2}, \quad (15)$$

and

$$a_{n,i} = \frac{\sigma_{T,i}^2}{\sigma_{n,i}^2}. \quad (16)$$

The following notation for the statistical quantities formed from vectors is followed here.

$$\text{Means:} \quad \langle \bar{X} \rangle = \sum_{i=1}^N a_i \bar{X}_i \quad (17)$$

$$\text{Covariances:} \quad \langle \bar{X} \bar{Y} \rangle = \langle \bar{X} \bar{Y}^T \rangle - \langle \bar{X} \rangle \langle \bar{Y}^T \rangle \quad (18)$$

where the superscript T denotes matrix transpose.

Minimizing $L_i(\bar{E}_i, \bar{G}_i, f_i)$ yields

$$\bar{E}_i^T \langle \bar{B}^R | \bar{B}^R \rangle_i - \bar{G}_i^T \langle \bar{D} | \bar{B}^R \rangle_i = \langle B_i | \bar{B}^R \rangle_i \quad (19a)$$

$$\bar{E}_i^T \langle \bar{B}^R | \bar{D} \rangle_i - \bar{G}_i^T \langle \bar{D} | \bar{D} \rangle_i = \langle B_i | \bar{D} \rangle_i \quad (19b)$$

$$f_i = \bar{E}_i^T \langle \bar{B}^R \rangle_i - \bar{G}_i^T \langle \bar{D} \rangle_i - \langle B_i \rangle_i \quad (19c)$$

where subscript i indicates that the averages are only over the i -th set. Equations (19a) and (19b) can be readily solved yielding:

$$\bar{E}_i^T = \left[\langle B_i | \bar{B}^R \rangle_i \langle \bar{D} | \bar{B}^R \rangle_i^{-1} - \langle B_i | \bar{D} \rangle_i \langle \bar{D} | \bar{D} \rangle_i^{-1} \right] \left[\langle \bar{B}^R | \bar{B}^R \rangle_i \langle \bar{D} | \bar{B}^R \rangle_i^{-1} - \langle \bar{B}^R | \bar{D} \rangle_i \langle \bar{D} | \bar{D} \rangle_i^{-1} \right]^{-1} \quad (20a)$$

$$\bar{G}_i^T = \left[\langle B_i | \bar{B}^R \rangle_i \langle \bar{B}^R | \bar{B}^R \rangle_i^{-1} - \langle B_i | \bar{D} \rangle_i \langle \bar{B}^R | \bar{D} \rangle_i^{-1} \right] \left[\langle \bar{D} | \bar{D} \rangle_i \langle \bar{B}^R | \bar{D} \rangle_i^{-1} - \langle \bar{D} | \bar{B}^R \rangle_i \langle \bar{B}^R | \bar{B}^R \rangle_i^{-1} \right]^{-1} \quad (20b)$$

f_i is then obtained by using Equations (20) in (19c).

RESULTS USING THE ROSSI X-RAY TIMING EXPLORER IN-FLIGHT DATA

Overview of the Mission and Data

The RXTE is an inertial-pointing spacecraft and was launched in December 1995 into a near-circular orbit of altitude 580 km and inclination 23 deg. The primary attitude sensors on board are charge-coupled device star trackers that provide accurate sensor-determined attitudes during inertial periods. The attitude during maneuvers (as many as eight each day) is obtained from accurately calibrated gyros. The predicted field values \bar{B} were generated using a 10th order IGRF model for the reference field values. Three sets of data from 1/4/96, 7/4/96, and 11/6/97 were used in the present study. Of these, the first two contain spacecraft slews (primarily about the z axis), while the last is wholly inertial. The telemetry data received at the FDF are nominally 2 sec apart, but various samples at a slower rate were generated to increase observability of the magnetic field variations. Thus, data were generated with pseudo-periods ranging from 4 sec to 40 sec, and several different telemetry periods were used for each set of data. However, the results presented here used 40 sec sampling for the 7/4/96 data and 8 sec sampling for the other two sets.

Terminology

Some notes about the figures and tables presented here are in order. The "truth" models used to evaluate the attitude and rate accuracies of the algorithms are the on-board computer (OBC) determined

attitudes and rates computed from their time derivatives. GCI-to-Body attitude results are presented in the form of 1-2-3 Euler angles, and these angles are respectively referred to as "Angle-1", " Angle-2", and " Angle-3". The body-frame components of the spacecraft rates are depicted in the figures as "wx", "wy", and "wz". "Raw" and "adjusted" refer to the quality of the TAM data, and denote pre- and post-calibration values for the TAM measurements. "Residuals" are the differences between TAM measurements and fields predicted using the RTSF attitude estimates. "TAM angle" is the angle between the measured and predicted fields. It is a convenient scalar parametrization of the separate TAM residuals along the three body axes and, as will be seen, is useful when evaluating the filter in the absence of truth models. Only TAM-1 measurements have been used throughout the paper although TAM-2 measurements are also available for the RXTE. The TAM-2 measurements and the residual statistics are not very different from the TAM-1 measurements, although significant differences do exist in the calibration parameters. "RTSF rate-errors " are the corrections, \bar{b} , estimated by the RTSF (see Equation (9)) as part of its state vector and are different from a term such as "error in wz" that refers to the differences between the RTSF rates and gyro rates. Thus \bar{b} may be viewed as "rate residuals" since convergence of the RTSF implies small \bar{b} .

TAM-1 Calibration Results

Excellent residual statistics were obtained after calibration of the data and the results are shown in Table 1 for each axis separately. For example, the root-mean-square residuals are of the order of 0.5 mG. The mean residuals are most impressive: of the order of 10^{-14} (i. e. of the order of "e-14" in the notation of the Table).

Table 1
RXTE RESIDUAL STATISTICS FOR TAM-1

Dataset	Pre-Calibration (Raw) Data (mG)		Post-Calibration (Adjusted) Data (mG)	
	Mean Residuals (X,Y,Z)	R-M-S Residuals (X,Y,Z)	Mean Residuals (X,Y,Z)	R-M-S Residuals (X,Y,Z)
1/4/96	4.105, -0.481, -1.792 Max: 9.290 Min: -6.949	4.720, 1.563, 3.191	-2e-14, -9e-15, -6e-14 Max: 3.019 Min: -1.296	0.519, 0.335, 0.272
7/4/96	3.055, -4.510, 3.413 Max: 7.984 Min: -3.196	3.162, 4.54, 4.114	2e-14, 2e-14, 4e-14 Max: 0.712 Min: -0.923	0.139, 0.216, 0.203
11/06/97	-1.561, -0.579, 8.221 Max: 15.670 Min: -6.635	2.778, 2.160, 9.085	7e-14, 7e-14, 2e-13 Max: 2.799 Min: -1.544	0.601, 0.312, 0.494

RTSF Tuning

The RTSF was tuned as follows. The largest of the r-m-s residuals results for a given dataset of Table 1 was used as the RTSF tuning parameter σ during the TAM-only runs; for example, this value would be 4.72 mG for the raw data of 1/4/96. At the outset of the TAM-only runs approximate numerical values for the filter propagation noise parameters, Q_a and Q_b of Equation (11), were obtained by analyzing the errors in the angular momentum of the spacecraft and wheels and the effects these errors would have on the RTSF rate and attitude while propagating between measurements. The uncertainties in the system net wheel

angular momentum was determined to be about 0.025 N-m, which resulted in rate uncertainties of 9.4×10^{-6} rad/sec. This implied Q_a was of the order of $10^{-10} \Delta t$ rad²/sec where Δt is the telemetry period. A related analysis using the convergence properties of the Markov model resulted in Q_b of the order of $2 \times 10^{-10} \Delta t$ rad²/sec³. Tuning was then accomplished by: (1) choosing a constant σ from Table 1 as stated above, (2) setting Q_a equal to Q_b during all of the runs, and (3) varying this adjustable single adjustable parameter $Q_{a,b}$ about the numerical value of $10^{-10} \Delta t$ until the attitude errors were minimized. The accuracy of the tuning parameters was verified later by studying the performance of the filter over several orders of magnitude of $Q_{a,b}$. For each dataset a few runs were also made using different σ but none yielded better performance. Each dataset was also studied using different telemetry periods. All in all a few *hundred* runs were made for each dataset, and only a small portion of the results are shown below.

A striking difference between the RTSF performance for RXTE and past experience with SAMPEX and ERBS data is the sensitivity to the numerical values of the numerical parameters, which in turn were somewhat dependent on the telemetry period. Thus, whereas it was sufficient for $Q_{a,b}$ to be accurate to one significant figure for SAMPEX and ERBS, it turns out that the tuning parameters have to be accurate to *three to four significant figures* for RXTE. As an example, for the 11/6/97 data with 8 sec telemetry period, the total RTSF attitude error was 15.6 deg when $Q_{a,b} = 1.1 \times 10^{-10}$ whereas this error dropped to 5.1 deg when $Q_{a,b} = 1.01 \times 10^{-10}$.

TAM-Only Results

DADMODO and RTSF (using IIC) attitude results for the 7/4/96 RXTE data with a telemetry period of 40 sec are presented in Fig. 1, which shows a spacecraft maneuver about the z-axis between 1500 sec and

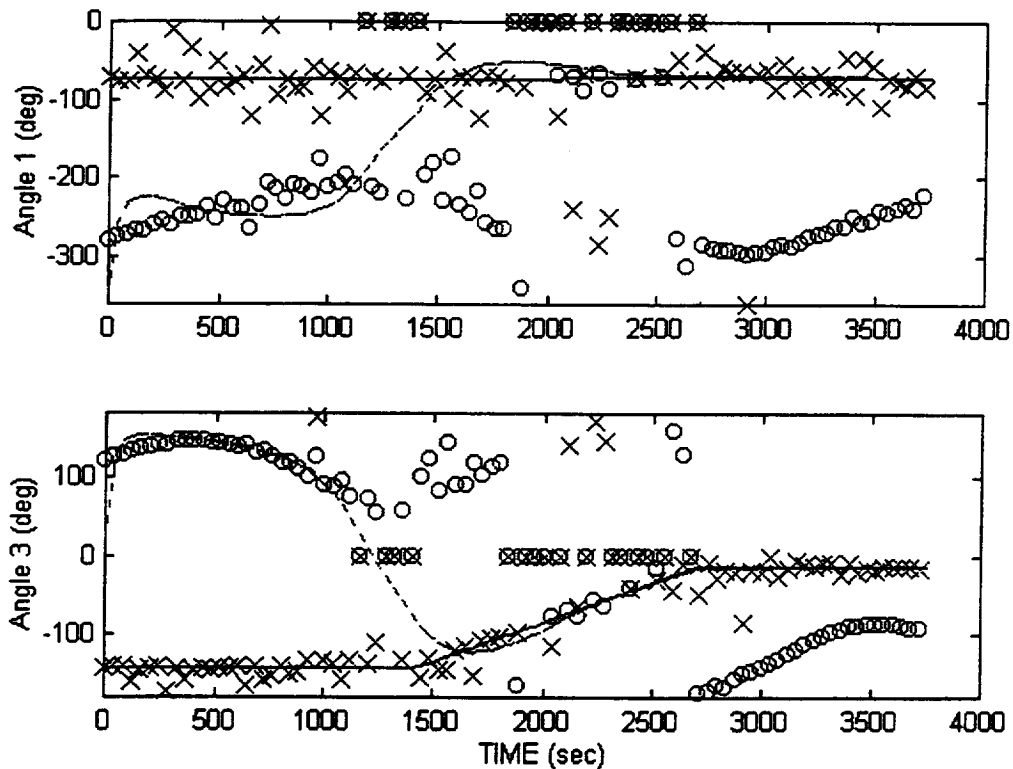


Figure 1. GCI-to-Body 1-2-3 Attitude Euler Angle Results for Adjusted 7/4/96 Data (solid = true, dashed = RTSF, crosses = DADMODO 1st root, circles = DADMODO 2nd root)

2500 sec. In this figure the lines represent the truth and the RTSF solutions (solid and dashed respectively) while the symbols represent the DADMOD correct and spurious solutions (crosses and circles respectively). The filter was started with IIC (large initial errors) and converged within 100 sec to a *metastable spurious* state that also shows up in the DADMOD solutions. The RTSF converges to the correct solution only about 1000 sec later—towards the start of the maneuver. This slow convergence of the filter is a direct result of the inertial-pointing nature of the spacecraft, which results in the orbital motion being the sole cause for changes in \bar{B} . (In fact, \bar{B}_i^R is approximately constant over the maneuver period.) *Note that: (1) this is the first independent confirmation of the DADMOD spurious solutions, and (2) such ambiguities will not arise if gyros provided the rate information and a TAM is used solely for attitude information. Note also a relatively large spread of the physical deterministic solution as a result of relatively low rate of change of \bar{B} .*

The slow convergence severely limits any rating of the accuracy of the filter: statistics for the last 15 points in Fig. 1 reveal r-m-s attitude errors of (0.43, 0.39, 0.17) deg about the three body axes. For more reliability, the filter was studied using data from the 1/4/96 dataset where an inertial span of nearly 4500 sec duration precedes the maneuver. The results are shown in Figs. 2 and 3.

Fig. 2 presents sample attitude and rate results for the 1/4/96 data of 8 sec telemetry period with the RTSF using IIC. These results were obtained with the numerical values of $Q_a = Q_b = 2.23 \times 10^{-11}$ and were deemed the optimal parameters after examining the error statistics. (See Table 2 below). We see that the filter converges by about 4000 sec even though the initial errors ranged from about 65 deg in Angle-3 to about 113 in Angle-1. Additional residual results from the same run are presented in Fig. 3. The RTSF state vector evolves so as to minimize all these quantities, and we see that all are small only after 4000 sec.

The convergence is slow here also, and it is instructive to examine the RTSF errors after 3200 sec separated into before, during, and after the maneuver. These are presented in the first and second columns of Table 2. Table 2 also compares these error statistics with the ones obtained using raw TAM data and a different set of tuning parameters ($Q_a = Q_b = 1.12 \times 10^{-9}$) separately determined to be optimal for the raw data. Some clear inferences can be drawn from examining Table 2.

- The attitude errors are significant before the maneuver but noticeably decrease during the maneuver, which we attribute to the increased observability of changes in \bar{B} .
- In contrast to the attitude errors, the errors in the rates *increase* during the maneuver, which we attribute to (small) dynamical modeling errors of the spacecraft.
- TAM calibration significantly improves TAM-only accuracies.

The above information is also seen qualitatively in the bottom plot of Fig. 2 and the middle and bottom plots of Fig. 3. Thus, Fig. 3 clearly shows us that the rates have converged well before the attitude; this is in accord with past experiences with the RTSF. It should be noted, though, that there will always be differences in the convergence times of the RTSF attitude and rate estimates because the rates are corrected based on the TAM residuals. Nevertheless, it would be interesting to examine in the future if better accuracies result from tuning Q_a and Q_b to yield the same convergence times for both attitude and rates.

The RTSF performance using IIC was further examined using the wholly inertial span of 11/6/97, IIC, and some of the results are shown in Fig. 4. It is clear (especially from the TAM angle plot) that the convergence time is of the order of 4400 sec. The error statistics from 4400 sec to the end of the data span are as follows:

$$\text{r-m-s attitude errors} = (0.54, 0.13, 0.33) \text{ deg}$$

$$\text{r-m-s errors in rates} = (0.0049, 0.0010, 0.0024) \text{ deg/sec}$$

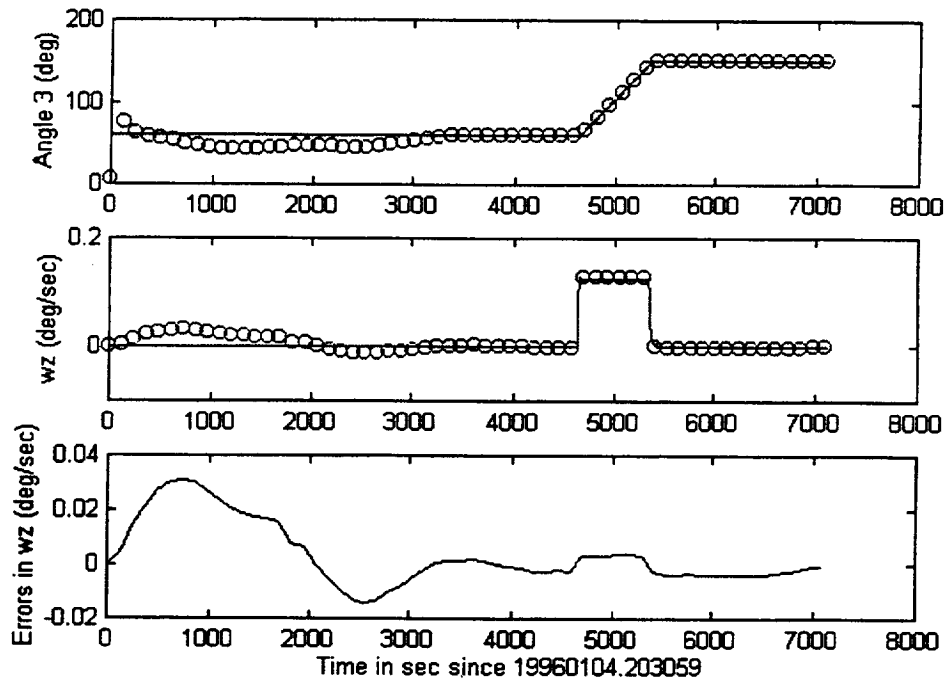


Figure 2. RTSF Attitude and Rate Results for Adjusted 1/4/96 Data (circles = RTSF and solid = truth in top two plots)

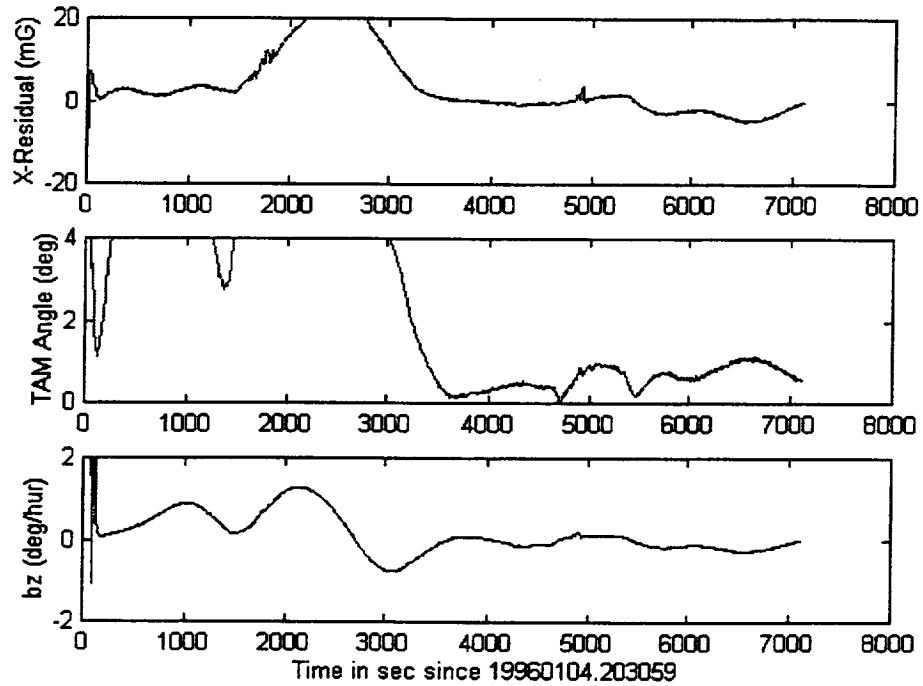


Figure 3. Additional RTSF Results for Adjusted 1/4/96 Data Showing TAM-1 Residuals (top two plots) and RTSF Rate-Error Estimates (bottom plot)

Table 2
RTSF ACCURACIES FOR 1/4/96 DATA SHOWING STATISTICS AFTER 3200 SEC

	Adjusted Data		Raw Data	
	R-M-S Attitude Errors (x, y, z) deg	R-M-S Errors in Rates (x, y, z) deg/sec	R-M-S Attitude Errors (x, y, z) deg	R-M-S Errors in Rates (x, y, z) deg/sec
Before	(1.15, 0.51, 0.68)	(0.0025, 0.0015, 0.0019)	(8.56, 2.37, 3.12)	(0.0099, 0.0035, 0.0075)
During	(0.70, 0.31, 0.36)	(0.0026, 0.0041, 0.0037)	(0.74, 1.09, 0.92)	(0.0023, 0.0073, 0.0030)
After	(0.38, 1.33, 0.65)	(0.0015, 0.0038, 0.0034)	(0.68, 2.06, 0.57)	(0.0017, 0.0043, 0.0033)

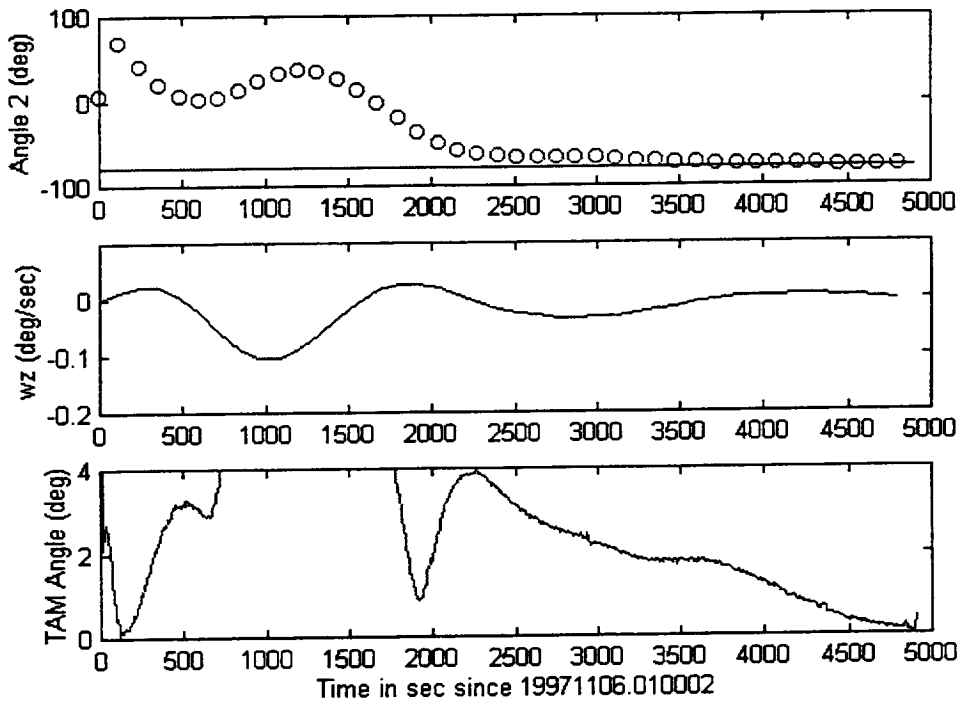


Figure 4. RTSF Results for Adjusted 11/6/97 Data (circles = filter in top plot)

CONCLUSIONS

In contrast to our past experiences with SAMPEX and ERBS, which were momentum-biased spacecraft spinning at the orbit rate, the RTSF performance for the zero-momentum, inertial-pointing RXTE is characterized by extreme sensitivity to filter tuning and long convergence times (about 4000 sec). Thus, while past SAMPEX and ERBS results demanded accuracies of only 1 significant figure in the tuning parameters, it was clear that accuracies of three to four significant figures were needed for success application to RXTE. The performance of both DADMOM and RTSF improved significantly once the

telemetry period was increased from the nominal value of 2 sec to between 8 and 40 sec. Presently we attribute this sensitivity to a combination of telemetry period and the zero-momentum nature of RXTE.

Careful tuning of the RTSF demonstrated per-axis attitude accuracies between 0.13 and 0.54 deg and rate accuracies between 0.0010 deg/sec and 0.0049 deg./sec when adjusted data were used. The corresponding values during the maneuver of 1/4/96 were 0.31 - 0.70 deg and to 0.0026 - 0.0041 deg/sec. These results are similar to our past results for ERBS⁸: attitude accuracies within 0.4 deg and rate accuracies within 0.005 deg/sec. We consider these accuracies preliminary in view of the long convergence times and the limited number of post-convergence results. More definitive accuracy studies are needed using long spans of inertial data. It would also be useful to study the relationship between the performance, the tuning, and the telemetry period.

Accurate TAM calibration was performed using a recently developed algorithm, and the subsequent RTSF TAM-only results show a significant improvement in the attitude accuracies upon using calibrated TAM data. This conclusion is in general agreement with studies using a TAM-gyro combination¹⁴.

An important theoretical development presented here is the transformation of a DADMOD transcendental equation into an 8th order polynomial. The first independent evidence of the accuracy of the DADMOD *spurious* solutions was obtained in the form of initial convergence of the RTSF to the metastable solution using the 4/7/96 data. To improve the DADMOD performance for inertial-pointing modes, a more sophisticated technique for smoothing time derivatives of the measured geomagnetic field should be applied to separate the physical root from the numerical noise.

REFERENCES

1. G. Natanson, S. McLaughlin, and R. Nicklas, "A Method of Determining Attitude From Magnetometer Data Only," *Proceedings of the Flight Mechanics/Estimation Theory Symposium 1990*, NASA Conference Publication 3102, Goddard Space Flight Center, Greenbelt, MD, May 1990
2. G. Natanson, J. Keat, and S. McLaughlin, *Sensor and Advanced Attitude Studies: Deterministic Attitude Computation Using Only Magnetometer Data*, Goddard Space Flight Center, Flight Dynamics Division, 554-FDD-91/010, prepared by Computer Sciences Corporation, March 1991
3. G. Natanson, "A Deterministic Method for Estimating Attitude From Magnetometer Data Only," Paper No. IAF-92-0036, *Proceedings of the World Space Congress*, Washington, DC, September 1992
4. M. Challa, *Solar, Anomalous, and Magnetospheric Particle Explorer (SAMPEX) Real Time Sequential Filter (RTSF): Evaluation Report*, Goddard Space Flight Center, Flight Dynamics Division, 553-FDD-93/024R0UD0, prepared by Computer Sciences Corporation, April 1993
5. M. Challa, G. Natanson, D. Baker, and J. Deutschmann, "Advantages of Estimating Rate Corrections During Dynamic Propagation of Spacecraft Rates—Applications to Real-Time Attitude Determination of SAMPEX," *Proceedings of the Flight Mechanics/Estimation Theory Symposium 1994*, NASA Conference Publication No. 3265, Goddard Space Flight Center, Greenbelt, MD, May 1994
6. G. Natanson, M. Challa, J. Deutschmann, and D. Baker, "Magnetometer-Only Attitude and Rate Determination for a Gyroless Spacecraft," *Proceedings of the Third International Symposium on Space Mission Operations and Ground Data Systems*, NASA Conference Publication 3281, Greenbelt, MD, November 1994, pp. 791–798.
7. M. Challa and G. Natanson, "A PC-Based Magnetometer-Only Attitude-and-Rate Determination System for Gyroless Spacecraft," *Proceedings of the Flight Mechanics and Estimation Theory Symposium*, NASA Conference Publication No. 3299, Goddard Space Flight Center, Greenbelt, MD, May 1995
8. M. Challa and C. Wheeler, "Accuracy Studies of a Magnetometer-Only Attitude-and-Rate Determination System," *Proceedings of the Flight Mechanics and Estimation Theory Symposium*, NASA Conference Publication No. 3333, Goddard Space Flight Center, Greenbelt, MD, May 1996

9. M. Challa, G. Natanson, and C. Wheeler, "Simultaneous Determination of Spacecraft Attitude and Rates Using Only a Magnetometer," *Proceedings of the American Institute of Aeronautics and Astronautics (AIAA)/American Astronautical Society (AAS) Astrodynamics Specialist Conference*, San Diego, CA, July 1996
10. M. Challa, S. Kotaru, and G. Natanson, "Magnetometer-Only Attitude and Rate Estimates During the Earth Radiation Budget Satellite 1987 Control Anomaly," *AIAA Guidance, Navigation and Control Conference*, New Orleans, August 11-13, 1997
11. J. Kronenwetter, M. Phenneger, and W. Weaver, "Attitude Analysis of the Earth Radiation Budget Satellite (ERBS) Yaw Turn Anomaly", *Proceedings of the Flight Mechanics/Estimation Theory Symposium*, NASA Conference Publication No. 3011, Goddard Space Flight Center, Greenbelt, MD, May 1988
12. M. Challa and R. Harman, "A New Magnetometer Calibration Algorithm and Application to the X-Ray Timing Explorer", *Proceedings of the AIAA Guidance, Navigation and Control Conference*, Boston, August 10-12, 1998 (to be published)
13. See, for example, the IGRF World Wide Web page at:
http://ftp.ngdc.noaa.gov/Solid_Earth/Mainfld_Mag/Models/
14. J. Hashmall and J. Deutschmann, "An Evaluation of Attitude-Independent Magnetometer-Bias Determination Methods", *Proceedings of the Flight Mechanics/Estimation Theory Symposium 1996*, NASA Conference Publication 3333, Goddard Space Flight Center, Greenbelt, MD, May 1996

